



Article

The Role of Surface Chemistry and Polyethylenimine Grafting in the Removal of Cr (VI) by Activated Carbons from Cashew Nut Shells

Victoria A. Smith ¹, Juster F. A. Rivera ¹, Ruby Bello ¹, Elena Rodríguez-Aguado ², Mohammed R. Elshaer ¹ ,
Rebecca L. Wodzinski ¹ and Svetlana Bashkova ^{1,*}

¹ Department of Chemistry, Biochemistry and Physics, Becton College of Arts and Sciences, Fairleigh Dickinson University, Madison, NJ 07940, USA; James_D@student.fdu.edu (V.A.S.); justeriv@student.fdu.edu (J.F.A.R.); ruby_b@student.fdu.edu (R.B.); melshaer@fdu.edu (M.R.E.); rwod@student.fdu.edu (R.L.W.)

² Departamento de Química Inorgánica, Facultad de Ciencias Universidad de Málaga, Campus de Teatinos, 29071 Málaga, Spain; aguadoelena5@gmail.com

* Correspondence: bashkova@fdu.edu

Abstract: Activated carbons prepared from cashew nut shells and modified by grafting polyethylenimine onto the surface were tested for removal of Cr (VI). The removal efficiency of carbons without and with polyethylenimine decreased with an increase in pH, with maximum efficiency found at pH 2. The average maximum adsorption capacities of carbons were calculated to be 340 ± 20 mg/g and 320 ± 20 mg/g for unmodified and modified carbons, respectively. Surface characterization of carbons revealed that C–O functionalities are actively involved in both polyethylenimine grafting and Cr (VI) removal. Moreover, lactone groups and amides, formed by polyethylenimine grafting, seemingly undergo acid hydrolysis with formation of phenol and carboxylic groups. Considering that Cr (III) is the only form of chromium found on the surface of both carbons, the reduction mechanism is deduced as the predominant one. Here Cr (VI), majorly present as HCrO_4^- , is attracted to the positively charged carbon surface, reduced to Cr (III) by phenol groups, and adsorbed inside the pores. The mechanism of Cr (VI) removal appears to be similar for unmodified and modified carbons, where the smaller adsorption capacity of the latter one can be related to steric hindrance and pore inaccessibility.

Keywords: activated carbon; adsorption capacity; cashew nut shells; chromium (VI) removal; polyethylenimine; surface chemistry



Citation: Smith, V.A.; Rivera, J.F.A.; Bello, R.; Rodríguez-Aguado, E.; Elshaer, M.R.; Wodzinski, R.L.; Bashkova, S. The Role of Surface Chemistry and Polyethylenimine Grafting in the Removal of Cr (VI) by Activated Carbons from Cashew Nut Shells. *C* **2021**, *7*, 27. <https://doi.org/10.3390/c7010027>

Received: 12 February 2021

Accepted: 24 February 2021

Published: 27 February 2021

Publisher's Note: MDPI stays neutral with regard to jurisdictional claims in published maps and institutional affiliations.



Copyright: © 2021 by the authors. Licensee MDPI, Basel, Switzerland. This article is an open access article distributed under the terms and conditions of the Creative Commons Attribution (CC BY) license (<https://creativecommons.org/licenses/by/4.0/>).

1. Introduction

Chromium water pollution is a serious environmental issue and is usually a result of human activities due to a poor industrial storage and inadequate waste disposal. The forms of chromium that most commonly occur in natural waters are trivalent chromium, Cr (III), and hexavalent chromium, Cr (VI). The former one is found in many food products and is essential in human dietary [1], whereas the latter one occurs naturally in rocks and soil, or is produced by industrial processes, such as tanning, metal plating, and welding. Cr (VI) is a more toxic form of chromium, which is non-biodegradable, and classified as a known carcinogen by the Environmental Protection Agency (EPA). According to Occupational Safety and Health Administration (OSHA), exposure to Cr (VI) may result in multiple adverse health effects, including asthma, eye damage, kidney and liver damage, pulmonary congestion and edema, and respiratory cancer [2]. EPA's drinking water standard for total chromium, including Cr (VI), is set to 0.1 ppm or 100 ppb. As stated by Environmental Working Group (EWG), based on the conducted laboratory tests, tap water of 31 out of 35 U.S. cities contains Cr (VI) [3]. According to EWG, at least 74 million people in nearly 7000

communities drink tap water polluted with “total chromium,” which includes hexavalent and other forms of the metal [3].

Most common treatment options for Cr (VI) include ion exchange [4,5], reverse osmosis [6], membrane separation process [7–9], reduction-precipitation [5,10], electrochemical processes [11,12], biosorption [13,14], and adsorption with activated carbon [15–30]. Amongst these methods, the advantages of using adsorption with activated carbon include method simplicity, cost-effectiveness, and ability for regeneration [1,19]. Furthermore, using activated carbons derived from agricultural waste products and other biomass waste such as waste palm trunk and mangrove provide an environmentally practical alternative, and a means of cutting costs while providing a solution for agricultural waste management [31–34]. Literature studies have shown that such agricultural waste precursors as corn straw [15], mango kernel [16], aloe vera waste leaves [19], Tamarind wood [20], Eichhornia crassipes root [21], peanut shell [22], apple peel [23], chestnut oak shell [24], longan seed [25], rice bran [26], and Zizibhus jujuba cores [27] can be successfully used for the production of activated carbons for Cr (VI) removal. Moreover, the modification of activated carbons by various methods can be employed to enhance their potential for removal of specific contaminants from aqueous phase [35]. Accordingly, several studies have shown that increasing the content of heteroatoms on the activated carbon surface may enhance Cr (VI) removal [36–42]. Thus, modification of activated carbon surface with long-chained nitrogen-containing polymer—polyethylenimine (PEI)—presents a viable perspective to improve the removal efficiency of carbon for chromium. Although limited data are published on Cr (VI) removal on activated carbons with PEI [41,42], the latter one was suggested to enhance the positive charge density of the carbon surface [36,41], which in turn can significantly increase the electrostatic affinity of Cr (VI), mostly present in solution as an anion [14,15,22,23,27–31,37,41,43].

The objectives of this research are to study the removal efficiencies of activated carbons from cashew nut shells for Cr (VI), and to explore the effect of PEI grafting. The focus of this study is to understand the role of surface functionality in the removal process, specifically the nature of participating surface functional groups. A thorough surface characterization of cashew nut shell based activated carbons before and after PEI grafting is performed in order to identify the mechanistic pathways of Cr (VI) removal.

2. Materials and Methods

2.1. Preparation of Activated Carbons from Cashew Nut Shells

95% n-hexane was purchased from Sigma-Aldrich[®], 85% o-phosphoric acid was purchased from Fisher Scientific[®]. Cashew oil was manually extracted from ground nut shells, by combining 20 g of the shells with 50 mL of hexane solvent, and leaving the mixture for 48 h. Shells were exposed to ambient air for 4 h and dried at 110 °C for 24 h. Impregnation with H₃PO₄ solution was done at 3.4:1 (H₃PO₄: shells) ratio by weight, while continuously stirring on a hot plate at ~85 °C for 2 h, followed by oven drying at 110 °C for 24 h. Carbonization of the impregnated shells was conducted in a horizontal tube furnace (Lindberg Blue M 1100C). The shells were heated to 400 °C at 20 mL/min under the inert atmosphere of nitrogen gas, and held at the final temperature for 2 h. Samples were then washed in Soxhlet extractors using 250 mL of deionized water until the pH of filtrate remained constant, and dried at 110 °C for 24 h. Resulting carbons were named as CNP, where letters stand for cashew, nut, and phosphoric acid.

2.2. Modification of Activated Carbons with PEI

Polyethylenimine (PEI), N-hydroxysuccinimide (NHS), methanol, and 1-Ethyl-3-(3-dimethylaminopropyl)carbodiimide (EDC) were purchased from Sigma-Aldrich[®] and Fischer Scientific[®]. A 200 mg portion of sieved CNP activated carbon was weighed out and added to a pristine 50 mL round bottom flask containing a magnetic stir bar. To this flask, 23.875 mL of methanol was added. The reaction mixture was stirred at 180 rpm at room temperature for several minutes. A 29 mg portion of NHS was dissolved in 700 µL of

methanol and then added to the reaction mixture. Several minutes later, 12 mg of EDC was dissolved in 300 μL of methanol and then also added. This mixture was stirred at room temperature for 30 min, and then 25 μL of 1800 MW PEI and 100 μL of triethylamine were added. This was stirred and stoppered for 48 h. The flask was then sonicated for 30 min and filtered by vacuum, followed by thorough washing with three portions of 25 mL of distilled water. This washing process was repeated for a total of three cycles. The modified carbon was then dried via vacuum filtration, collected, and weighed. Modified carbon is designated as CNP PEI.

2.3. Cr(VI) Batch Adsorption Studies

0.1 N hydrochloric acid (HCl) and potassium dichromate ($\text{K}_2\text{Cr}_2\text{O}_7$) powder were purchased from Sigma-Aldrich[®]. To study the effect of pH on the removal efficiency of Cr (VI), solutions of 10, 40 and 100 mg/L of Cr (VI) were prepared. Each solution was separated into aliquots, and each aliquot adjusted to a different pH level within the range of 2 to 5, using 0.1 N HCl. Then, 20 mL of each aliquot was mixed with 12.5 mg of the activated carbon sample, previously sieved to 250 μm particle size. These mixtures were shaken for 24 h at 175 rpm on a compact digital mini rotator (Thermo Scientific), and filtered, using size 12.5 cm filter paper. The absorbance of each filtrate was measured using direct UV-Vis spectrometry [44] at ~ 350 nm (red shift is observed at a higher pH) with Olis 8453 UV-Visible Spectrophotometer (Olis Data). The equilibrium concentrations of the filtrate solutions were calculated from the absorbance values using external standard calibration ($Q_L = 0.2$ ppm and $R^2 = 1.0000$ at 10-100 ppm of Cr (VI)). The removal efficiency of carbons was calculated as:

$$\text{Removal efficiency \%} = \frac{(C_0 - C_e)}{C_0} \times 100 \quad (1)$$

where C_0 is the initial concentration of Cr (VI) solution in mg/L, and C_e is the concentration of Cr (VI) at equilibrium in mg/L.

To calculate the adsorption capacities of carbon samples at different pH levels, the solutions of Cr (VI) in the concentration range of 10–200 mg/L were prepared. Each solution was adjusted to pH 2 and mixed with the carbon sample. Here the same procedure as for the study of the effect of pH was followed. The experimental equilibrium data were fit to Langmuir (Equation (2)) and Freundlich (Equation (3)) isotherm models.

$$q_e = \frac{Q_m K_L C_e}{1 + K_L C_e} \quad (2)$$

$$q_e = K_F C_e^{\frac{1}{n}} \quad (3)$$

where Q_m is the maximum adsorption capacity (mg/g); K_L is the Langmuir adsorption constant (L/mg); K_F is the Freundlich adsorption constant ((mg/g)(L/mg)^{1/n}); n is a constant related to the favorability of adsorption.

The amount of Cr(VI) adsorbed at equilibrium q_e (mg/g) was calculated by Equation (4)

$$q_e = \frac{(C_0 - C_e)V}{m} \quad (4)$$

where V is the volume of Cr (VI) solution in L and m is the mass of carbon adsorbent in g.

2.4. Fourier Transform Infrared (FT-IR) Spectroscopy

FT-IR spectra were obtained on a Nicolet iS10 FT-IR Spectrometer (Thermo Fisher Scientific[®]), using ATR attachment. The spectrum was collected 50 times in the wavenumber range between 4000 and 400 cm^{-1} and corrected for the background noise.

2.5. X-Ray Photoelectron Spectroscopy (XPS)

XPS studies were performed on a Physical Electronic spectrometer (PHI Versa Probe II) using monochromatic Al K α radiation (52.8 W, 15 kV, 1486.6 eV) and a dual beam charge neutralizer for analyzing the core-level signals of the elements of interest with a hemispherical multichannel detector. The activated carbon sample spectra were recorded with a constant pass energy value at 29.35 eV and a beam diameter of 100 μ m. Energy scale was calibrated using Cu 2p $_{3/2}$, Ag 3d $_{5/2}$, and Au 4f $_{7/2}$ photoelectron lines at 932.7, 368.2, and 83.95 eV, respectively. The X-ray photoelectron spectra obtained were analyzed using PHI SmartSoft software and processed using MultiPak 9.6.0.15 package. The binding energy values were referenced to C1s signal at 284.5 eV. Shirley-type background and Gauss-Lorentz curves were used to determine the binding energies. Atomic concentration percentages of the characteristic elements were determined considering the corresponding area sensitivity factor for the different measured spectral regions.

2.6. X-Ray Diffraction (XRD)

Laboratory X-ray powder diffraction (XRPD) patterns were collected on a PANanalytical EMPYREAN automated diffractometer. Powder patterns were recorded in Bragg-Brentano reflection configuration by using the PIXcel 3D detector with a step size of 0.017 $^\circ$ (2 θ). The powder patterns were recorded between 5 and 70 in 2 θ with a total measuring time of 10 min.

2.7. pH of Carbon Surface

Activated carbon powder (0.1 g) was placed in 5 mL of de-ionized water and equilibrated overnight at 175 rpm. Then pH of the suspension was measured using a Piccolo ATC pH tester (Hanna Instruments).

3. Results and Discussion

The effect of pH on the removal efficiency of Cr (VI) was studied for CNP and CNP PEI at three different concentrations of Cr (VI)—10, 40 and 100 mg/L (Figure 1). The results in the pH range of ~2 to 5 show that with the increase in pH, the removal efficiency of carbons decreases. Both CNP and CNP PEI display similar behavior based on the average data collected from multiple batches of carbons (Figure 1). The maximum in removal efficiency is detected at solution pH of ~2, which is in agreement with the results obtained by other researchers [16,19,22,28,41]. It is suggested that HCrO $_4^-$, which is the predominant form of Cr (VI) at pH 2, is electrostatically attracted to the positively charged carbon surface, causing an increase in its removal by the activated carbon. On the other hand, as the pH of solution increases, more negatively charged species are present (Cr $_2$ O $_7^{2-}$, CrO $_4^{2-}$, OH $^-$), all of which compete for the adsorption sites, causing the electrostatic repulsion of chromium species from the carbon surface. It is also noticeable from Figure 2 that the removal efficiencies of carbons are higher at lower concentrations. Thus, at 10 mg/L of Cr (VI) the maximum removal efficiency is on average observed up to pH 4. At higher concentrations, the active adsorption sites of carbon are quickly saturated with chromium species, which results in a faster decrease of removal efficiency of carbons with the increase in pH.

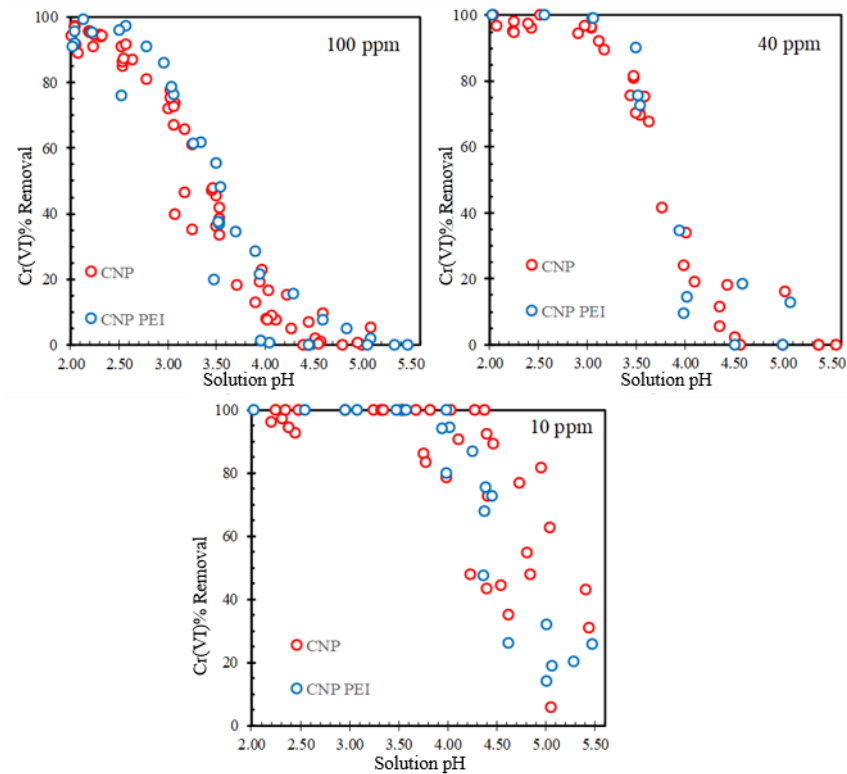


Figure 1. Removal efficiencies of CNP and CNP PEI carbons in the pH range of 2 to 5 at the concentration of Cr (VI) of 10 mg/L, 40 mg/L and 100 mg/L.

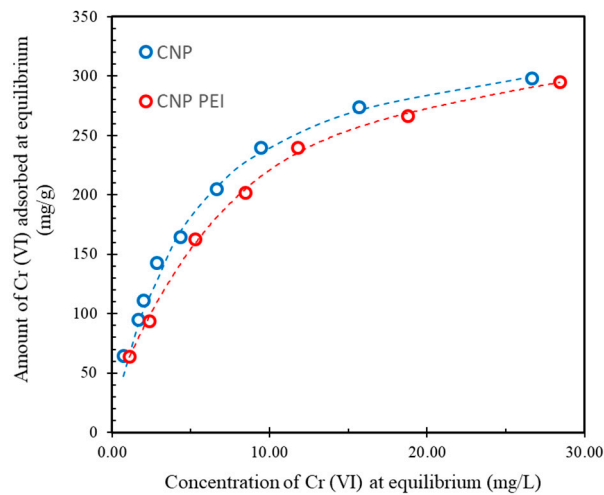


Figure 2. Langmuir isotherms for Cr (VI) adsorption on CNP and CNP PEI carbons, measured at pH 2.

The Langmuir and Freundlich adsorption models were applied to the experimental equilibrium data collected at solution pH of ~ 2 for 10–200 mg/L of Cr (VI), and the Langmuir model was found to have a better fit for both CNP and CNP PEI carbons (Table 1 and Figure 2), indicating a homogeneous monolayer adsorption of Cr (VI) on the carbon surface. Herein the Langmuir model was used to calculate the maximum adsorption capacity, Q_m , and the average Q_m values for seven batches of CNP carbon with and without the PEI are presented in Table 1; shown with their corresponding confidence intervals at 95% confidence level (CI). In addition, the surface pH values are also given in Table 1, where the surface pH increases after PEI grafting, due to the introduction of amine groups onto the carbon surface, and decreases after Cr (VI) removal on both CNP and CNP PEI, indicating changes in the surface chemistry of carbons.

Table 1. pH of the carbon surface and isotherm parameters for Cr (VI) adsorption on CNP and CNP PEI at solution pH of ~ 2.

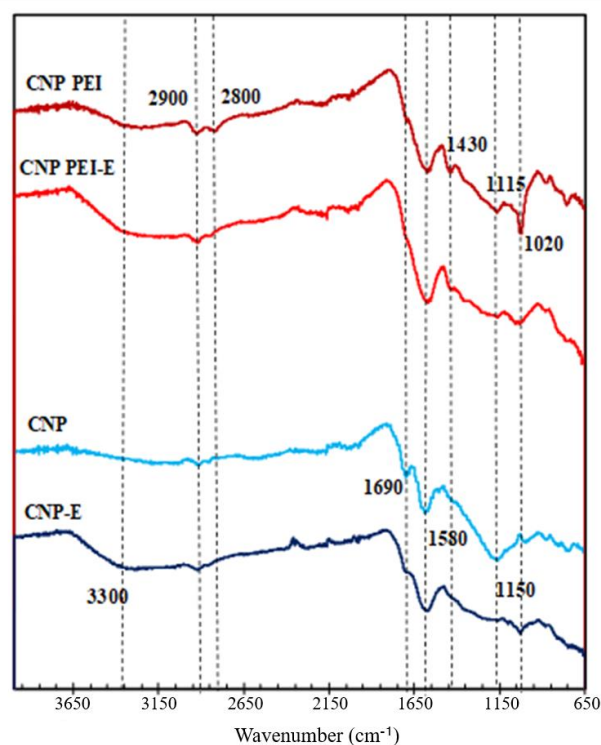
Sample	pH/pH E ¹	Langmuir			Freundlich		
		Q _m ± CI (mg/g)	K _L (L/mg)	R ²	K _F (mg/g)(L/mg) ^{1/n}	1/n	R ²
CNP	2.9/2.5	340 ± 20	0.19	0.9981	97.3	0.27	0.9481
CNP PEI	3.5/2.8	320 ± 20	0.17	0.9991	98.4	0.34	0.9810

¹ "E" stands for exhausted carbon—after chromium removal at solution pH ~2 and 100 mg/L.

In general, the capacity values for Cr (VI) on both CNP and CNP PEI carbons in Table 1 are at a higher range of those reported for similar materials in literature. Only a few capacity values reported were found to exceed the ones in this work, i.e., 401.5 mg/g for PEI aerobic granules [45], 435.7 mg/g for PEI-alkali biochar [46], 539.53 mg/g for PEI-graphene oxide [47]; these values however were obtained at a higher concentration range (>100 mg/g) of Cr (VI).

The results in Table 1 show that the adsorption capacity of CNP is somewhat higher than that of CNP PEI. To understand this trend, a detailed surface evaluation is further conducted, since surface functionality is expected to play a vital role in the removal of Cr (VI) [1,16,23,28,37,43]. The surface functional groups are known to attract chromium species to the carbon surface, where they can be further stored inside the carbon's pores. However, grafting PEI onto the surface may result in surface being overloaded with functional groups, which may cause steric hindrance and pore inaccessibility, and therefore, lower the adsorption capacity of carbon.

To obtain a better understanding of the processes taking place on the carbon surface and the effect of surface functionality on the removal of chromium species, carbons were analyzed by FT-IR, XPS and XRD analyses. The results of FT-IR analysis are presented in Figure 3. Here, E denotes the exhausted carbons, i.e., carbons after chromium removal at solution pH of ~2 and 100 mg/L Cr (VI).

**Figure 3.** FTIR spectra of CNP and CNP PEI and their exhausted counterparts.

For initial CNP carbon, multiple bands are detected, which reflect a rich surface chemistry of this carbon. Thus, the broad band at $\sim 3300\text{ cm}^{-1}$ is characteristic of a stretching vibration of hydrogen-bonded (O–H) hydroxyl groups from carboxyl, phenol, alcohol, or surface bonded water [31,41,48–51]. For CNP carbon grafted with PEI (CNP PEI) it is also associated with the N–H stretch [36,41,49–52]. Two small bands at ~ 2900 and 2800 cm^{-1} , especially visible on the spectra of PEI modified sample, correspond to C–H stretching vibrations [41,51]. The band at $\sim 1690\text{ cm}^{-1}$ for CNP is related to C=O stretching vibration in carboxylic acids [48,49,52]. Furthermore, this band for CNP PEI shifts to 1670 cm^{-1} , and may be associated with N–H bend in amines or amides [36,48,51]. The band at $\sim 1580\text{ cm}^{-1}$ of CNP is assigned to aromatic ring stretching coupled to highly conjugated carbonyl groups [31,48]. For CNP PEI, just like in the case of the band at 1690 cm^{-1} , the band at 1580 cm^{-1} may also be associated with the N–H bend [48]. The overlap of multiple broad absorption bands happens in the region of $\sim 1400\text{--}1000\text{ cm}^{-1}$, commonly attributed to C–O stretching in acid, alcohol, phenol, ether and/or ester groups, and phosphorous containing functionalities, P=O/P–O, due to the activation with phosphoric acid [41,48,50]. The bands at 1115 , 1020 and 1430 cm^{-1} for CNP PEI may denote the C–N stretching vibration [19,41]. Any bands below 950 cm^{-1} are due to out-of-plane deformation vibrations of C–H groups in aromatic structures or may also be associated with the N–H wag in amines [19,48].

Upon removal of Cr (VI), the most noticeable spectral differences are observed in the regions of 3300 and $1400\text{--}1000\text{ cm}^{-1}$. The intensity of the 3300 cm^{-1} band increases, suggesting the formation of new hydroxyl groups, and the intensity of the peak centered at 1150 cm^{-1} significantly decreases, implying active participation of C–O and P=O/P–O functionalities in the removal process.

For CNP PEI sample, the formation of bands at 2900 , 2800 , 1430 and 1020 cm^{-1} along with the increased intensity of bands at 3300 and 1580 cm^{-1} affirm the successful grafting of PEI on the surface; the bands at 1670 and 1580 cm^{-1} may also denote the formation of C=O containing groups upon grafting. More so, the shift of 1150 cm^{-1} band for CNP to 1115 cm^{-1} for CNP PEI suggests the involvement of C–O functionalities in the grafting of PEI. After chromium removal, the decrease in the intensities of bands at 1115 , 1020 and 1430 cm^{-1} is the most noticeable, indicating the involvement of C–N functionalities in the removal process. On the other hand, some increase in the magnitude of bands at 3300 , 1690 and 1580 cm^{-1} imply the formation of O–H and C=O containing groups upon chromium removal.

To shed more light on the importance of different functional groups in the removal of Cr (VI), the carbons with and without the PEI were further analyzed by XPS. The results of this analysis are presented in Table 2 and Figures 4–8. For C 1s spectrum (Figure 4), significant changes are observed in the region of $\sim 285.8\text{ eV}$ associated with C–O bonds in phenols, esters and ethers [48,53], and C–N bonds [41,50,54]. The amount of these groups increased by $\sim 22\%$ after PEI grafting, supporting the appearance of C–N containing functionalities, and decreased after Cr (VI) removal (by $\sim 30\%$ for CNP and by $\sim 40\%$ for CNP PEI), indicating the involvement of C–O and C–N groups in the removal process. These findings are in agreement with FT–IR results (Figure 3). On the other hand, the increase in C=O functionalities is noted for the exhausted carbons. This is affirmed by the elevated intensity of a peak at $\sim 287.1\text{ eV}$ (by $\sim 56\%$ for CNP and by $\sim 42\%$ for CNP PEI), assigned to carbonyl groups [48,53], and the appearance of a peak at $\sim 288.1\text{ eV}$ ascribed to C=O in carboxylic and carbonyl groups [50,54]. Furthermore, the increase in the intensity of C 1s peak at $\sim 289.1\text{ eV}$ is detected for CNP PEI. This contribution is associated with O–C=O in carboxylic/ester and N–C=O in amide groups [41,48,54], suggesting their formation, particularly amides, upon PEI grafting.

Table 2. Results of the deconvolution of the XPS spectra for C 1s, O 1s, P 2p, Cr 2p, and N 1s and the element content in atomic % (bold letters) for the initial and exhausted “E” CNP carbon with and without PEI.

Binding Energy eV	Bond Assignment	CNP %	CNP-E %	CNP PEI %	CNP PEI-E %
C 1s		89.68	78.29	79.61	78.35
284.5	C–C (sp ² carbon)	71.48	66.51	63.03	65.63
285.8 ± 0.2	C–O (phenol, ester, ether)/C–N	17.78	12.25	22.95	13.43
287.1 ± 0.4	C=O (carbonyl)	5.30	12.04	6.43	11.10
288.1 ± 0.1	C=O (carboxyl/carbonyl)		4.82		6.43
289.1 ± 0.4	O–C=O (carboxyl, ester)/ N–C=O	3.89	3.22	5.56	2.09
290.8 ± 0.1	π - π^*	1.55	1.16	2.02	1.33
O 1s		9.59	19.91	11.68	18.50
531.4 ± 0.3	O=C (carbonyl, ester)/O=C–N	36.09	34.39	67.41	37.25
532.9 ± 0.1	O–C (phenol, ether, ester, carboxyl)	63.91	65.61	32.59	62.75
P 2p		0.73	0.56	0.64	0.46
133.2 ± 0.1	phosphate	100	100	100	100
Cr 2p			1.24		0.83
577.3	Cr (III)		67.67		65.77
586.9 ± 0.1	Cr (III)		32.33		34.23
N 1s				8.06	1.87
399.9 ± 0.2	amine/amide			100	100

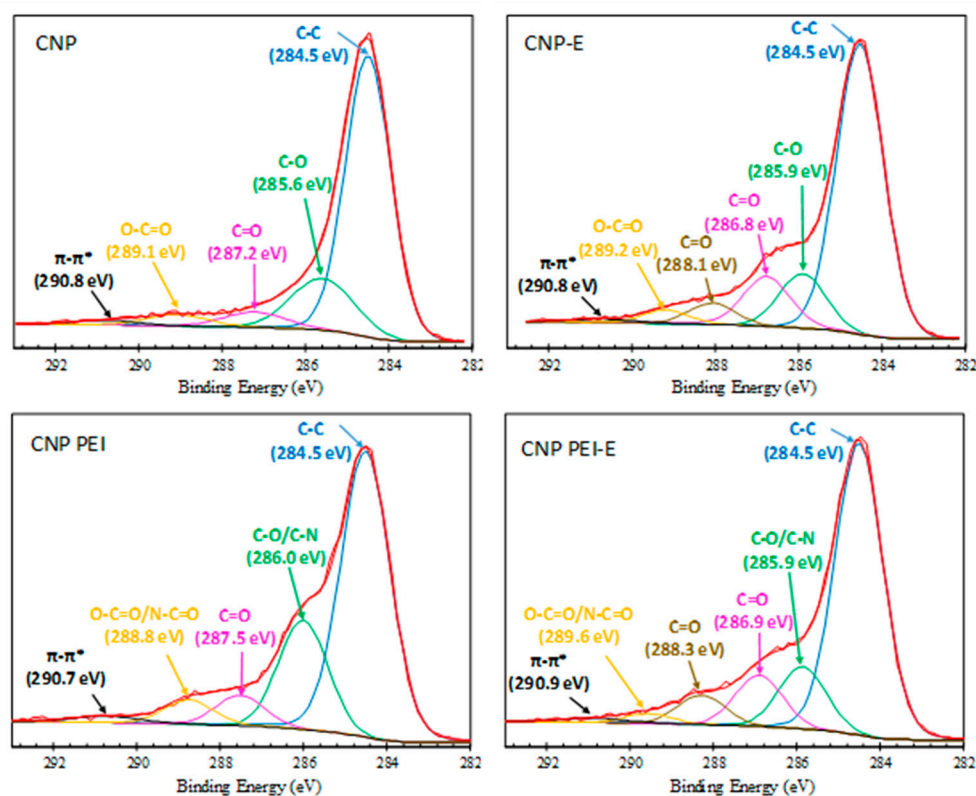


Figure 4. C 1s XPS spectra of CNP, CNP-E, CNP PEI, CNP PEI-E.

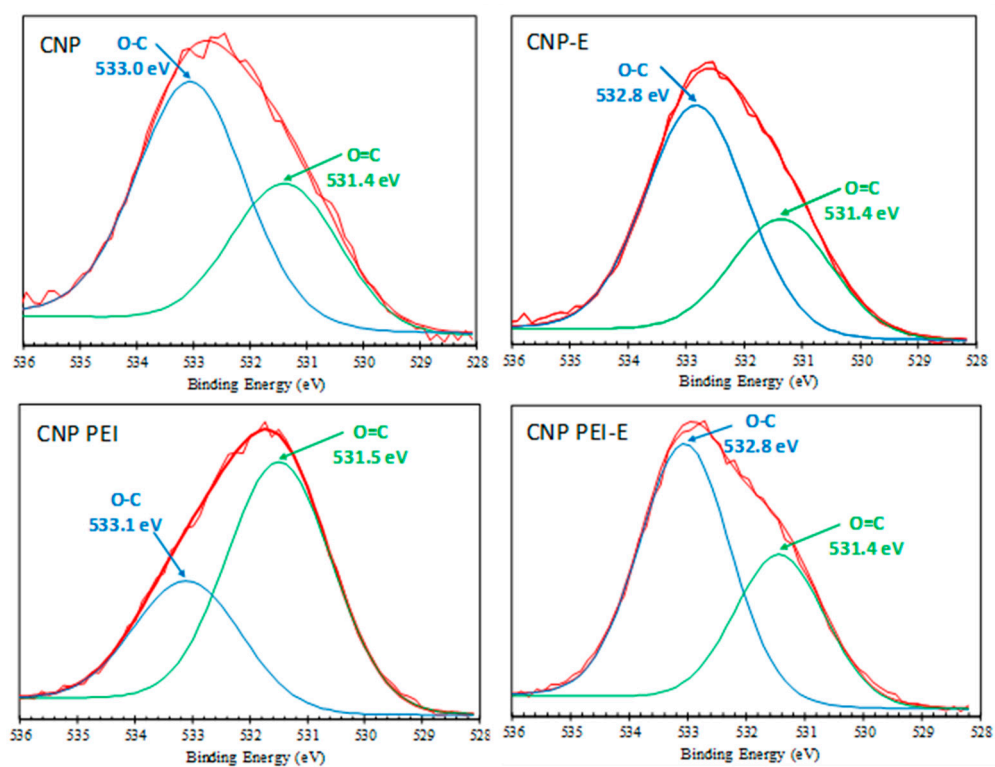


Figure 5. O 1s XPS spectra of CNP, CNP-E, CNP PEI, CNP PEI-E.

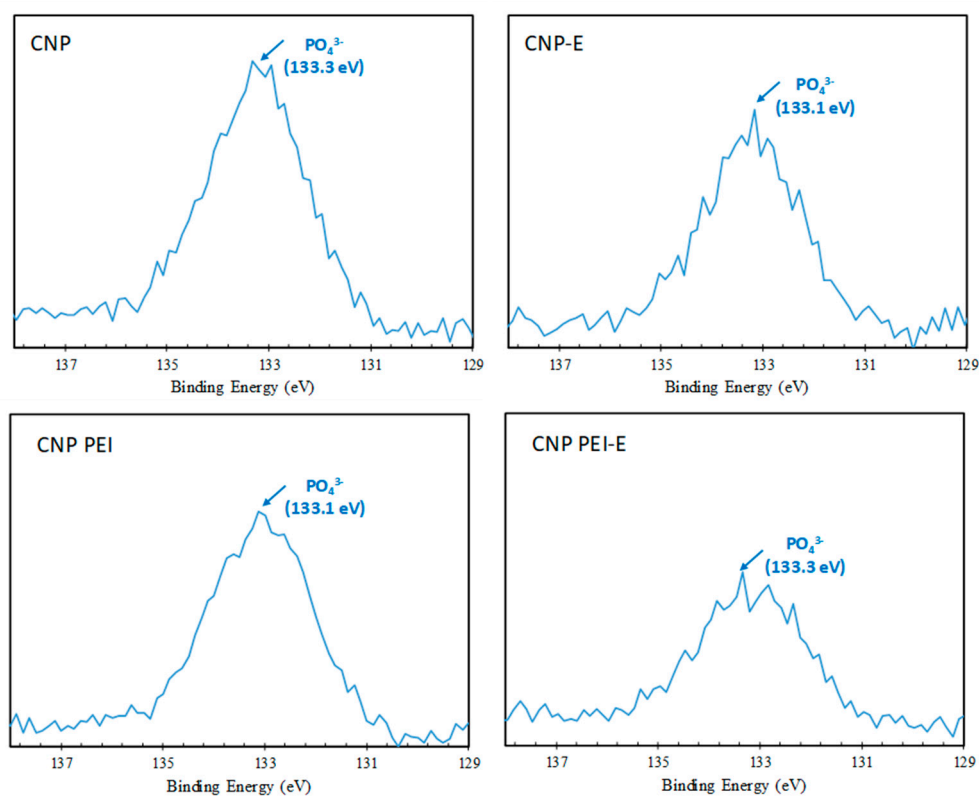


Figure 6. P 2p XPS spectra of CNP, CNP-E, CNP PEI, CNP PEI-E.

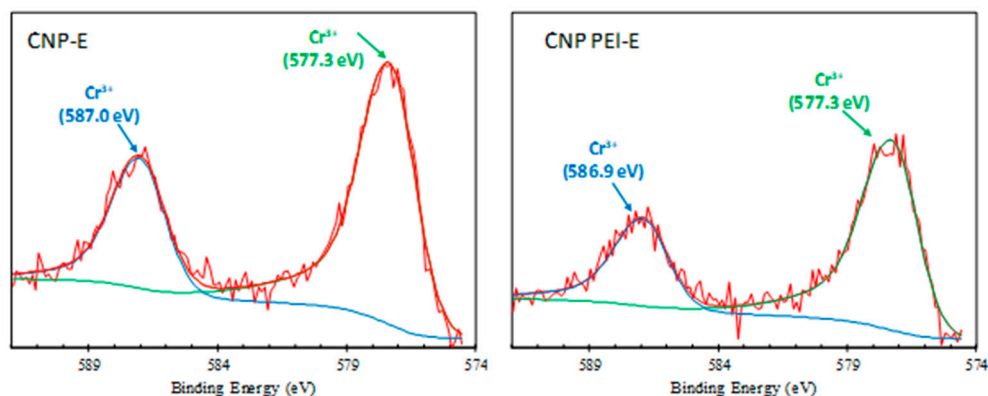


Figure 7. Cr 2p XPS spectra of CNP-E and CNP PEI-E.

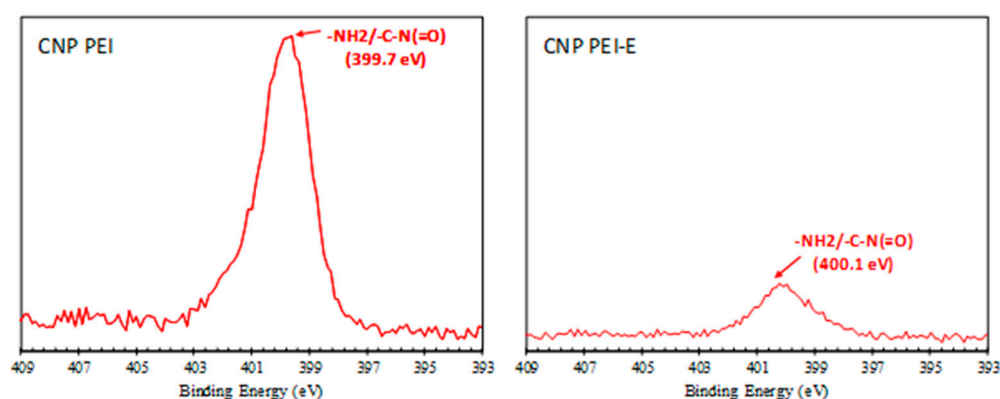


Figure 8. N 1s XPS spectra of CNP PEI and CNP PEI-E.

The evaluation of O 1s spectra (Figure 5) shows the appearance of two contributions, at ~ 531.4 and ~ 532.9 eV, where the former one is assigned to O=C in carbonyl/ester and/or amide groups [48,54], and the latter one to O–C functionalities in phenol, ether, ester, and carboxylic groups [54]. Interestingly, O–C groups predominate on the surface of CNP by $\sim 44\%$ over O=C groups, but it is completely the opposite for CNP PEI, where O=C groups are prevalent by $\sim 52\%$. This suggests that the O–C groups participate in the PEI grafting, producing O=C/O=C–N groups on the surface. Furthermore, the amount of O=C/O=C–N functionalities decreases by $\sim 45\%$ after chromium removal, which implies that they are actively involved, whereas the amount of O–C groups increases by 48%.

Phosphate functionalities are detected on the surface of CNP and CNP PEI by the presence of P 2p peak of ~ 133.2 eV (Figure 6); phosphate arises from the activation of cashew nut shells with phosphoric acid. The amount of phosphate decreases upon PEI grafting and chromium removal, indicating its effective participation in both processes.

Deconvolution of Cr 2p spectra results in a doublet Cr 2p_{3/2}–Cr 2p_{1/2} at 577.3/586.9 eV (Figure 7). This doublet corresponds to Cr (III) species [50], which form on the surface of CNP and CNP PEI carbons as a result of Cr (VI) reduction. It is noteworthy that the amount of Cr (III) on the surface of CNP and CNP PEI carbons appears to be about the same, with a somewhat lower amount of Cr (III) found on the latter one.

As a confirmation of a successful grafting of PEI, a N 1s peak at 399.7 eV is observed for CNP PEI (Figure 8). The peak at this binding energy is related to the presence of amines and amides [41,48,51,54]. The intensity of this peak decreases significantly after chromium removal, affirming the participation of amine/amide groups in the removal process.

To provide some insight into the crystalline structure of the surface, carbon samples with and without the PEI were analyzed by XRD. The XRD powder diffractograms of the initial and exhausted samples are presented in Figure 9. The reflections at 24° and 43° correspond to d_{002} and d_{100} respectively, and indicate the presence of turbostratic structure

or random layer lattice structure [15,40,55]. The diffraction peak at 24° corresponds to a d-spacing of 0.37 nm, which could be attributed to the presence of a variety of oxygen containing functionalities [53]. The intensity of this peak decreases substantially after PEI grafting, suggesting the loss of crystallinity and pore filling by PEI [56]. More so, a small peak at 22.8° , to the left of the main peak at 24° , is commonly described as a γ -band and is related to the presence of aliphatic sidechains at the edges of crystallites [55]. Similarly, the peak at 11.3° on CNP PEI can be ascribed to the introduction of functional groups onto the basal planes [57]. The diffractograms of the exhausted carbons exhibit similar patterns with the decreased intensity of the peak at 24° . This decrease can be associated with the reduced crystallinity and pore filling with chromium species. Interestingly, the peaks at 22.8° and 11.3° on CNP PEI disappear after chromium removal, signifying the engagement of PEI functionalities in the removal process.

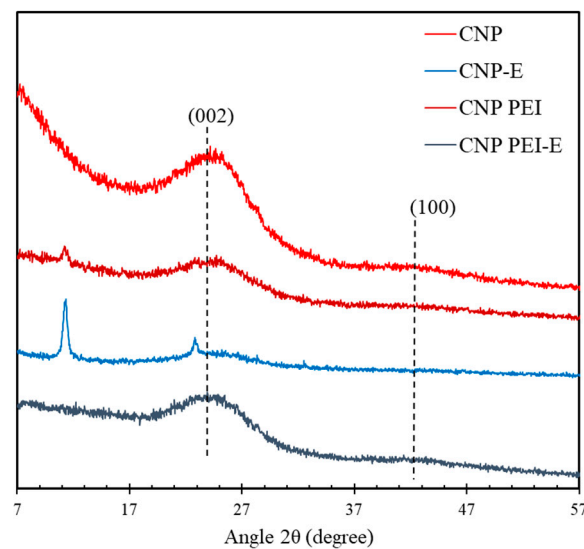
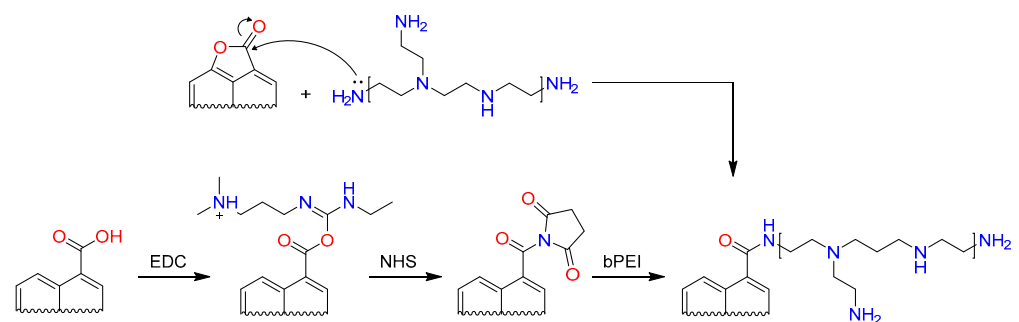


Figure 9. XRD plots of CNP and CNP PEI and their exhausted counterparts.

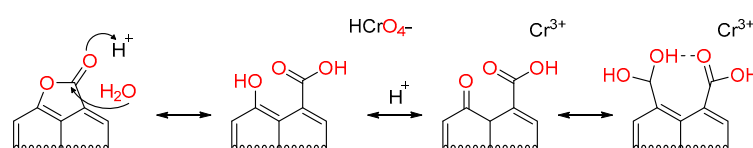
Based on the detailed surface analysis conducted in this study, the possible mechanisms of PEI grafting on the surface of CNP, and Cr (VI) removal by CNP and CNP PEI carbons can be derived.

PEI grafting involves oxygen-containing groups on the carbon surface. According to our previous study [48], the potentiometric titration of CNP carbon prepared at 400°C showed that the majority of these groups are lactones, followed by carboxylic acids and phenols. Thus, lactones may undergo nucleophilic attack at the carbonyl group by PEI amines, thereby forming phenols and amide linkages (Scheme 1). Similarly, the mechanism of PEI grafting via carbodiimide EDC/NHS coupling of carboxylic surface groups with PEI amines results in the formation of amide groups (Scheme 1).



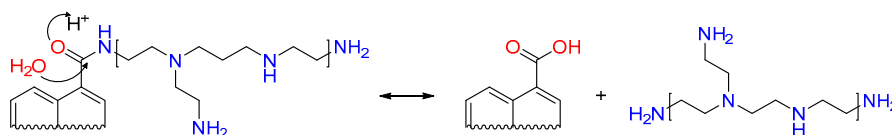
Scheme 1. PEI grafting on the surface of CNP.

For the removal of Cr (VI) on the CNP carbon without PEI, the surface analyses were conducted for the testing conditions of pH 2. In such acidic conditions, the majority of lactone groups are expected to undergo acid catalyzed ester hydrolysis to form carboxylic and phenol groups on the surface (Scheme 2). Furthermore, chromium, which is mostly present in the form of HCrO_4^- (at pH of ~ 2) is electrostatically attracted to the positively charged carbon surface [19–28,30,39,43,50], reduced to Cr (III) (the only form of chromium detected by XPS (Table 2 and Figure 7)), and adsorbed inside the carbon pores. The detailed analysis of textural parameters of cashew nut shell-based activated carbons prepared by chemical activation with phosphoric acid was previously conducted [48], and carbons were found to have a high surface area ($>1000 \text{ m}^2/\text{g}$) and well developed porosity (volume of pores more than $1 \text{ cm}^3/\text{g}$, and volume of micropores more than $0.1 \text{ cm}^3/\text{g}$). At the same time, some phenol surface groups are oxidized to form carboxylic acids and additional carbonyl/quinone groups on the surface, which can further dimerize when in close proximity to each other [48].



Scheme 2. Acid catalyzed hydrolysis of lactone groups, followed by Cr (VI) reduction to Cr (III).

In the case of Cr (VI) removal on CNP PEI, amides may also undergo acid hydrolysis in strongly acidic conditions with the formation of carboxyl groups on the surface (Scheme 3). Thus, the pH of the filtrate solution (after separation of exhausted carbon from solution) went up to pH ~ 3 from the original pH ~ 2 of chromium solution, indicating the possible presence of amines in the solution after chromium removal.



Scheme 3. Acid catalyzed hydrolysis of amide groups.

It is noteworthy that the only form of chromium detected by XPS on the surface of both CNP and CNP PEI carbons is Cr (III) (Table 2 and Figure 7), strongly demonstrating the prevalence of reduction mechanism in Cr (VI) removal, and eliminating the possibility of Cr (VI) complexation with amine groups of PEI. Therefore, just like in the case of CNP, the removal of Cr (VI) on CNP PEI occurs by the mechanism outlined in Scheme 2—reduction of Cr (VI) to Cr (III) by phenol groups and their subsequent oxidation to carbonyls and carboxylic acids.

From here we can conclude that the removal efficiency of both CNP and CNP PEI carbons depends on the presence of positive surface charge, phenol groups on the surface, and well developed porosity. The amount of phenol groups on CNP PEI may be somewhat lower than that on CNP as some $-\text{OH}$ groups may H-bond with amines of PEI, making them unavailable to chromium species. In addition, despite the large surface area and well-developed porosity of CNP carbon [48], the high density of its oxygen containing groups [48] with addition of imine functionalities causes group dimerization, which lowers pore accessibility and initiates steric hindrance [48]. This prevents Cr (III) from being adsorbed inside the carbon pores, which could explain the lower average adsorption capacity of CNP PEI than that of CNP (Table 1).

4. Conclusions

In this work, activated carbons were prepared from cashew nut shells by chemical activation with phosphoric acid. These carbons were further modified by grafting

polyethylenimine onto their surface. Hereafter, both unmodified and modified carbons were tested for removal of Cr (VI). The pH tests for Cr (VI) removal showed that the removal efficiency of both carbons decreased with an increase in pH from 2 to 5, with the maximum removal efficiency found at pH 2. The average maximum adsorption capacities of carbons, calculated based on the Langmuir adsorption model were found to be 340 ± 20 mg/g and 320 ± 20 mg/g for unmodified and PEI modified carbons, respectively.

Detailed surface characterization of carbons by FT-IR, XPS and XRD analyses showed that C–O type functionalities are actively involved in both PEI grafting and Cr (VI) removal processes. The grafting of PEI apparently proceeds via the formation of amide linkages on the surface. Moreover, lactone groups, which are the most abundant on CNP, and amides, formed upon PEI grafting, are expected to undergo acid hydrolysis in strongly acidic conditions of pH 2. Here phenol and carboxylic groups are formed as a result of these processes.

Considering that Cr (III) is the only form of chromium found on the surface of both unmodified and PEI modified carbons, the reduction mechanism is deduced as the predominant one. In summary, Cr (VI), which is mostly present in the form of HCrO_4^- at pH 2, is attracted to the positively charged carbon surface, reduced to Cr (III) by phenol groups primarily (phenol groups are in turn oxidized to produce carbonyl and carboxylic groups), and adsorbed inside the carbon pores. Although, the mechanism of Cr (VI) removal appears to be similar for both carbons, the PEI modified carbon exhibits somewhat smaller average adsorption capacity. This decrease in capacity upon PEI grafting can mostly be related to the surface being saturated with functional groups, which can lead to dimerization, and consecutively cause steric hindrance, restricting the accessibility of chromium to carbon pores.

Author Contributions: Conceptualization, S.B.; methodology, S.B., E.R.-A., R.L.W., and M.R.E.; software, S.B. and E.R.-A.; validation, S.B., V.A.S., J.F.A.R., R.B., M.R.E., R.L.W., and E.R.-A.; formal analysis, S.B. and E.R.-A.; investigation, S.B., V.A.S., J.F.A.R., R.B., R.L.W., and E.R.-A.; resources, S.B., M.R.E. and E.R.-A.; data curation, S.B.; writing—original draft preparation, S.B.; writing—review and editing, S.B., E.R.-A., M.R.E., J.F.A.R., V.A.S., and R.B.; visualization, S.B.; supervision, S.B.; project administration, S.B.; funding acquisition, S.B., E.R.-A. All authors have read and agreed to the published version of the manuscript.

Funding: This research was funded by RTI2018-099668-BC22 of Ministerio de Ciencia, Innovación y Universidades, and project UMA18-FEDERJA-126 of Junta de Andalucía and FEDER funds.

Institutional Review Board Statement: Not Applicable.

Data Availability Statement: Not Applicable.

Acknowledgments: This work was supported by Grant-In-Aid Program and the Department of Chemistry, Biochemistry and Physics at Fairleigh Dickinson University. Authors are grateful to Vincent Menafro for experimental help.

Conflicts of Interest: The authors declare no conflict of interest. The funders had no role in the design of the study; in the collection, analyses, or interpretation of data; in the writing of the manuscript, or in the decision to publish the results.

References

1. Pakade, V.E.; Tavengwa, N.T.; Madikizela, L.M. Recent advances in hexavalent chromium removal from aqueous solutions by adsorptive methods. *RSC Adv.* **2019**, *9*, 26142–26164. [CrossRef]
2. Health Effects of Hexavalent Chromium. OSHA Fact Sheet, (July 2006). Available online: https://www.osha.gov/OshDoc/data_General_Facts/hexavalent_chromium.html (accessed on 20 February 2021).
3. EWG (Environmental Working Group). Chromium-6 Is Widespread in US Tap Water. 2009. Available online: <https://www.ewg.org/research/chromium6-in-tap-water> (accessed on 20 February 2021).
4. Cavaco, S.A.; Fernandes, S.; Quina, M.M.; Ferreira, L.M. Removal of chromium from electroplating industry effluents by ion exchange resins. *J. Hazard. Mater.* **2007**, *144*, 634–638. [CrossRef]

5. Ye, Z.; Yin, X.; Chen, L.; He, X.; Lin, Z.; Liu, C.; Ning, S.; Wang, X.; Wei, Y. An integrated process for removal and recovery of Cr(VI) from electroplating wastewater by ion exchange and reduction–precipitation based on a silica-supported pyridine resin. *J. Clean. Prod.* **2019**, *236*, 117631. [[CrossRef](#)]
6. Mousavi Rad, S.A.; Mirbagheri, S.A.; Mohammadi, T. Using reverse osmosis membrane for chromium removal from aqueous solution. *Int. Schol. Sci. Res. Innov.* **2009**, *3*, 505–509.
7. Modrzejewska, Z.; Kaminski, W. Separation of Cr(VI) on Chitosan Membranes. *Ind. Eng. Chem. Res.* **1999**, *38*, 4946–4950. [[CrossRef](#)]
8. Yao, Z.; Du, S.; Zhang, Y.; Zhu, B.; Zhu, L.; John, A.E. Positively charged membrane for removing low concentration Cr(VI) in ultrafiltration process. *J. Water Process. Eng.* **2015**, *8*, 99–107. [[CrossRef](#)]
9. Khulbe, K.C.; Matsuura, T. Removal of heavy metals and pollutants by membrane adsorption techniques. *Appl. Water Sci.* **2018**, *8*, 19. [[CrossRef](#)]
10. Wójcik, G.; Wieszczycka, K.; Aksamitowski, P.; Zembrzuska, J. Elimination of carcinogenic chromium(VI) by reduction at two-phase system. *Sep. Purif. Technol.* **2020**, *238*, 116410. [[CrossRef](#)]
11. Jin, W.; Du, H.; Zheng, S.; Zhang, Y. Electrochemical processes for the environmental remediation of toxic Cr(VI): A review. *Electrochim. Acta* **2016**, *191*, 1044–1055. [[CrossRef](#)]
12. Maitlo, H.A.; Kim, K.-H.; Park, J.Y.; Kim, J.H. Removal mechanism for chromium (VI) in groundwater with cost-effective iron-air fuel cell electrocoagulation. *Sep. Purif. Technol.* **2019**, *213*, 378–388. [[CrossRef](#)]
13. Vieira, M.; Osirovici, R.; Gimenes, M.; Silva, M. Biosorption of chromium(VI) using a Sargassum sp. packed-bed column. *Bioresour. Technol.* **2008**, *99*, 3094–3099. [[CrossRef](#)]
14. Jobby, R.; Jha, P.; Yadav, A.K.; Desai, N. Biosorption and biotransformation of hexavalent chromium [Cr(VI)]: A comprehensive review. *Chemosphere* **2018**, *207*, 255–266. [[CrossRef](#)] [[PubMed](#)]
15. Ma, H.; Yang, J.; Gao, X.; Liu, Z.; Liu, X.; Xu, Z. Removal of chromium (VI) from water by porous carbon derived from corn straw: Influencing factors, regeneration and mechanism. *J. Hazard. Mater.* **2019**, *369*, 550–560. [[CrossRef](#)] [[PubMed](#)]
16. Rai, M.; Shahi, G.; Meena, V.; Meena, R.; Chakraborty, S.; Singh, R.; Rai, B. Removal of hexavalent chromium Cr (VI) using activated carbon prepared from mango kernel activated with H₃PO₄. *Resour. Technol.* **2016**, *2*, S63–S70. [[CrossRef](#)]
17. Wang, Y.; Peng, C.; Padilla-Ortega, E.; Robledo-Cabrera, A.; López-Valdivieso, A. Cr(VI) adsorption on activated carbon: Mechanisms, modeling and limitations in water treatment. *J. Environ. Chem. Eng.* **2020**, *8*, 104031. [[CrossRef](#)]
18. Valentín-Reyes, J.; García-Reyes, R.; García-González, A.; Soto-Regalado, E.; Cerino-Córdova, F. Adsorption mechanisms of hexavalent chromium from aqueous solutions on modified activated carbons. *J. Environ. Manag.* **2019**, *236*, 815–822. [[CrossRef](#)]
19. Prajapati, A.K.; Das, S.; Mondal, M.K. Exhaustive studies on toxic Cr(VI) removal mechanism from aqueous solution using activated carbon of Aloe vera waste leaves. *J. Mol. Liq.* **2020**, *307*, 112956. [[CrossRef](#)]
20. Acharya, J.; Sahu, J.; Sahoo, B.; Mohanty, C.; Meikap, B. Removal of chromium(VI) from wastewater by activated carbon developed from Tamarind wood activated with zinc chloride. *Chem. Eng. J.* **2009**, *150*, 25–39. [[CrossRef](#)]
21. Giri, A.K.; Patel, R.; Mandal, S. Removal of Cr (VI) from aqueous solution by Eichhornia crassipes root biomass-derived activated carbon. *Chem. Eng. J.* **2012**, *185–186*, 71–81. [[CrossRef](#)]
22. Al-Othman, Z.; Ali, R.; Naushad, M. Hexavalent chromium removal from aqueous medium by activated carbon prepared from peanut shell: Adsorption kinetics, equilibrium and thermodynamic studies. *Chem. Eng. J.* **2012**, *184*, 238–247. [[CrossRef](#)]
23. Enniya, I.; Rghioui, L.; Jourani, A. Adsorption of hexavalent chromium in aqueous solution on activated carbon prepared from apple peels. *Sustain. Chem. Pharm.* **2018**, *7*, 9–16. [[CrossRef](#)]
24. Niazi, L.; Lashanizadegan, A.; Sharififard, H. Chestnut oak shells activated carbon: Preparation, characterization and application for Cr (VI) removal from dilute aqueous solutions. *J. Clean. Prod.* **2018**, *185*, 554–561. [[CrossRef](#)]
25. Yang, J.; Yu, M.; Chen, W. Adsorption of hexavalent chromium from aqueous solution by activated carbon prepared from longan seed: Kinetics, equilibrium and thermodynamics. *J. Ind. Eng. Chem.* **2015**, *21*, 414–422. [[CrossRef](#)]
26. Singh, K.; Rastogi, R.; Hasan, S. Removal of Cr(VI) from wastewater using rice bran. *J. Colloid Interface Sci.* **2005**, *290*, 61–68. [[CrossRef](#)]
27. Labied, R.; Benturki, O.; Hamitouche, A.Y.E.; Donnot, A. Adsorption of hexavalent chromium by activated carbon obtained from a waste lignocellulosic material (Ziziphus jujuba cores): Kinetic, equilibrium, and thermodynamic study. *Adsorpt. Sci. Technol.* **2018**, *36*, 1066–1099. [[CrossRef](#)]
28. Miretzky, P.; Cirelli, A.F. Cr(VI) and Cr(III) removal from aqueous solution by raw and modified lignocellulosic materials: A review. *J. Hazard. Mater.* **2010**, *180*, 1–19. [[CrossRef](#)] [[PubMed](#)]
29. Attia, A.A.; Khedr, S.A.; Elkholy, S.A. Adsorption of chromium ion (VI) by acid activated carbon. *Braz. J. Chem. Eng.* **2010**, *27*, 183–193. [[CrossRef](#)]
30. Solgi, M.; Najib, T.; Ahmadnejad, S.; Nasernejad, B. Synthesis and characterization of novel activated carbon from Medlar seed for chromium removal: Experimental analysis and modeling with artificial neural network and support vector regression. *Resour. Technol.* **2017**, *3*, 236–248. [[CrossRef](#)]
31. Spagnoli, A.A.; Giannakoudakis, D.A.; Bashkova, S. Adsorption of methylene blue on cashew nut shell based carbons activated with zinc chloride: The role of surface and structural parameters. *J. Mol. Liq.* **2017**, *229*, 465–471. [[CrossRef](#)]
32. Pal, A.; Uddin, K.; Saha, B.B.; Thu, K.; Kil, H.-S.; Yoon, S.-H.; Miyawaki, J. A benchmark for CO₂ uptake onto newly synthesized biomass-derived activated carbons. *Appl. Energy* **2020**, *264*, 114720. [[CrossRef](#)]

33. Pal, A.; Uddin, K.; Thu, K.; Saha, B.B.; Kil, H.-S.; Yoon, S.-H.; Miyawaki, J. Synthesis of High Grade Activated Carbons From Waste Biomass. In *Renewable and Sustainable Materials*, 1st ed.; Elsevier BV: Amsterdam, The Netherlands, 2020; Volume 4, pp. 584–595. [[CrossRef](#)]
34. Pal, A.; Uddin, K.; Thu, K.; Saha, B.B.; Kil, H.-S.; Yoon, S.-H.; Miyawaki, J. Thermophysical and Adsorption Characteristics of Waste Biomass-Derived Activated Carbons. In *Renewable and Sustainable Materials*, 1st ed.; Elsevier BV: Amsterdam, The Netherlands, 2020; Volume 4, pp. 617–628. [[CrossRef](#)]
35. Bhatnagar, A.; Hogland, W.; Marques, M.; Sillanpää, M. An overview of the modification methods of activated carbon for its water treatment applications. *Chem. Eng. J.* **2013**, *219*, 499–511. [[CrossRef](#)]
36. Sun, J.; Zhang, Z.; Ji, J.; Dou, M.; Wang, F. Removal of Cr⁶⁺ from wastewater via adsorption with high-specific-surface-area nitrogen-doped hierarchical porous carbon derived from silkworm cocoon. *Appl. Surf. Sci.* **2017**, *405*, 372–379. [[CrossRef](#)]
37. Valix, M.; Cheung, W.; Zhang, K. Role of heteroatoms in activated carbon for removal of hexavalent chromium from wastewaters. *J. Hazard. Mater.* **2006**, *135*, 395–405. [[CrossRef](#)]
38. Fang, J.; Gu, Z.; Gang, D.; Liu, C.; Ilton, E.S.; Deng, B. Cr(VI) Removal from Aqueous Solution by Activated Carbon Coated with Quaternized Poly(4-vinylpyridine). *Environ. Sci. Technol.* **2007**, *41*, 4748–4753. [[CrossRef](#)] [[PubMed](#)]
39. Li, P.; Hu, M.; Suo, J.; Xie, Y.; Hu, W.; Wang, X.; Wang, Y.; Zhang, Y. Enhanced Cr(VI) removal by waste biomass derived nitrogen/oxygen co-doped microporous biocarbon. *Environ. Sci. Pollut. Res.* **2019**, *27*, 5433–5445. [[CrossRef](#)]
40. Chen, F.; Zhang, M.; Ma, L.; Ren, J.; Ma, P.; Li, B.; Wu, N.; Song, Z.; Huang, L. Nitrogen and sulfur codoped micro-mesoporous carbon sheets derived from natural biomass for synergistic removal of chromium(VI): Adsorption behavior and computing mechanism. *Sci. Total. Environ.* **2020**, *730*, 138930. [[CrossRef](#)]
41. Chen, S.; Wang, J.; Wu, Z.; Deng, Q.; Tu, W.; Dai, G.; Zeng, Z.; Deng, S. Enhanced Cr(VI) removal by polyethylenimine- and phosphorus-codoped hierarchical porous carbons. *J. Colloid Interface Sci.* **2018**, *523*, 110–120. [[CrossRef](#)]
42. Owlad, M.; Aroua, M.K.; Daud, W.M.A.W. Hexavalent chromium adsorption on impregnated palm shell activated carbon with polyethyleneimine. *Bioresour. Technol.* **2010**, *101*, 5098–5103. [[CrossRef](#)]
43. Islam, A.; Angove, M.J.; Morton, D.W. Recent innovative research on chromium (VI) adsorption mechanism. *Environ. Nanotechnol. Monit. Manag.* **2019**, *12*, 100267. [[CrossRef](#)]
44. Sanchez-Hachair, A.; Hofmann, A. Hexavalent chromium quantification in solution: Comparing direct UV–visible spectrometry with 1,5-diphenylcarbazide colorimetry. *Comptes Rendus Chim.* **2018**, *21*, 890–896. [[CrossRef](#)]
45. Sun, X.-F.; Ma, Y.; Liu, X.-W.; Wang, S.-G.; Gao, B.-Y.; Li, X.-M. Sorption and detoxification of chromium(VI) by aerobic granules functionalized with polyethylenimine. *Water Res.* **2010**, *44*, 2517–2524. [[CrossRef](#)]
46. Ma, Y.; Liu, W.-J.; Zhang, N.; Li, Y.-S.; Jiang, H.; Sheng, G.-P. Polyethylenimine modified biochar adsorbent for hexavalent chromium removal from the aqueous solution. *Bioresour. Technol.* **2014**, *169*, 403–408. [[CrossRef](#)] [[PubMed](#)]
47. Chen, J.H.; Xing, H.T.; Guo, H.X.; Weng, W.; Hu, S.R.; Li, S.X.; Huang, Y.H.; Sun, X.; Su, Z.B. Investigation on the adsorption properties of Cr(vi) ions on a novel graphene oxide (GO) based composite adsorbent. *J. Mater. Chem. A* **2014**, *2*, 12561–12570. [[CrossRef](#)]
48. Geczo, A.; Giannakoudakis, D.A.; Triantafyllidis, K.; Elshaer, M.R.; Rodríguez-Aguado, E.; Bashkova, S. Mechanistic insights into acetaminophen removal on cashew nut shell biomass-derived activated carbons. *Environ. Sci. Pollut. Res.* **2020**, 1–14. [[CrossRef](#)]
49. Ren, Z.; Xu, X.; Wang, X.; Gao, B.; Yue, Q.; Song, W.; Zhang, L.; Wang, H. FTIR, Raman, and XPS analysis during phosphate, nitrate and Cr(VI) removal by amine cross-linking biosorbent. *J. Colloid Interface Sci.* **2016**, *468*, 313–323. [[CrossRef](#)]
50. Bandara, P.C.; Peña-Bahamonde, J.; Rodrigues, D.F. Redox mechanisms of conversion of Cr(VI) to Cr(III) by graphene oxide-polymer composite. *Sci. Rep.* **2020**, *10*, 1–8. [[CrossRef](#)]
51. Guo, H.; Jiao, T.; Zhang, Q.; Guo, W.; Peng, Q.; Yan, X. Preparation of Graphene Oxide-Based Hydrogels as Efficient Dye Adsorbents for Wastewater Treatment. *Nanoscale Res. Lett.* **2015**, *10*, 1–10. [[CrossRef](#)] [[PubMed](#)]
52. Moreno-Castilla, C.; López-Ramón, M.; Carrasco-Marín, F. Changes in surface chemistry of activated carbons by wet oxidation. *Carbon* **2000**, *38*, 1995–2001. [[CrossRef](#)]
53. Lyu, H.; Tang, J.; Huang, Y.; Gai, L.; Zeng, E.Y.; Liber, K.; Gong, Y. Removal of hexavalent chromium from aqueous solutions by a novel biochar supported nanoscale iron sulfide composite. *Chem. Eng. J.* **2017**, *322*, 516–524. [[CrossRef](#)]
54. Kehrner, M.; Duchoslav, J.; Hinterreiter, A.; Cobet, M.; Mehic, A.; Stehrer, T.; Stifter, D. XPS investigation on the reactivity of surface imine groups with TFAA. *Plasma Process. Polym.* **2019**, *16*, 1800160. [[CrossRef](#)]
55. Manoj, B.; Kunjomana, A.G. Study of stacking structure of amorphous carbon by X-Ray diffraction technique. *Int. J. Electro-chem. Sci.* **2012**, *7*, 3127–3134.
56. Xu, X.; Song, C.; Andresen, J.M.; Miller, B.G.; Scaroni, A.W. Novel Polyethylenimine-Modified Mesoporous Molecular Sieve of MCM-41 Type as High-Capacity Adsorbent for CO₂ Capture. *Energy Fuels* **2002**, *16*, 1463–1469. [[CrossRef](#)]
57. Park, J.; Kim, Y.S.; Sung, S.J.; Kim, T.; Park, C.R. Highly dispersible edge-selectively oxidized graphene with improved electrical performance. *Nanoscale* **2016**, *9*, 1699–1708. [[CrossRef](#)] [[PubMed](#)]